Radarsat observations and forecasting of oil slick trajectory movements

Maged Marghany

(Institute of Oceanography(INOS), University College Science and Technology Malaysia(KUSTEM), 21030 Mengabnag Telipot, Kuala Terengganu, Malaysia. E-mail: magedupm@hotmail.com; mmm@kustem.edu.my)

Abstract: RADARSAT data have a potential role for coastal pollution monitoring. This study presents a new approach to detect and forecast oil slick trajectory movements. The oil slick trajectory movements is based on the tidal current effects and Fay's algorithm for oil slick spreading mechanisms. The oil spill trajectory model contains the integration between Doppler frequency shift model and Lagrangian model. Doppler frequency shift model implemented to simulate tidal current pattern from RADARSAT data while the Lagrangian model used to predict oil spill spreading pattern. The classical Fay's algorithm was implemented with the two models to simulate the oil spill trajectory movements.

The study shows that the slick lengths are effected by tidal current V component with maximum velocity of 1.4 m/s. This indicates that oil slick trajectory path is moved towards the north direction. The oil slick parcels are accumulated along the coastline after 48 h. The analysis indicated that tidal current V components were the dominant forcing for oil slick spreading.

Keywords: RADARSAT data; oil spill trajectory movements; marine oil pollution; Malacca Straits

Introduction

Marine oil pollution and its impact on marine ecosystems is a great matter along the coastal waters. An excellent understanding of the oil slick spreading mechanisms will be more useful to marine environmental protection. To avoid a great oil pollution crisis along the coastal waters, the radar remote sensing could be good tool for detecting and controlling oil slick spreading. Synthetic Aperture Radar(SAR) data have a significant role in remote sensing based slick detection. SAR data are depicted excellent results for oil spill detection. According to Bern et al. (Bern, 1992) the visibility concept of the oil slick in SAR image function of the reduced radar backscatter from the surface. The oil spills appear as dark patches on SAR imaged. The backscatter is function on the wind speed. There are several assumptions for oil slick detection. These assumptions include that: (1) the higher probability for the occurrence of oil spill can be observed close to bright object in SAR image. The bright object could be ship or platform; (2) the oil spill can be observed in SAR image by the discrimination with the surroundings sea. The heterogeneous surroundings mean that the oil slick spots are separated from the surroundings based on contrast(Wahl, 1993; Anne, 1999).

There are several studies have been carried attention to the wind effects on imagine oil slick by SAR. The different pattern of wind speeds probably create spatial variation of radar backscatter along the image. It was found that there is no backscatter from undisturbed sea surface with 0 m/s of wind speed, hence there is no signature of oil slicks. The wind speed of 3 m/s induces the slightly roughened sea surface. It seems that there is no impact from the wind on the oil slick. This provides an area of local low wind appears as dark patches. This dark patches may be interpreted as oil slick look-alikes. Researchers have agreed that oil spill will be visible in SAR images with wind speed lager than 3 m/s. As the matter of fact, the combination of oil spill dispersion will be function of the oil type, wave breaking, and velocity bunching. Velocity bunching is primarily a wave height and wave period driven mechanisms. In general, oil slick can be visible in SAR images with dark spot at wind speed higher than 7 m/s, while look-alikes are visible at wind speed 3 m/s(Wesiteen, 1993; Hovland, 1994; Wahl, 1993; Anne, 1999; Benelli, 1999; Maged, 2000).

However, the full potential capacity of SAR application to coastal pollution studies has not been implemented yet. There are no many studies have been used SAR for oil slick trajectory monitoring. This is because of the fact that an excellent understanding to the oil slick trajectory is important for early warning and contingency plan. It can not be ignored the classical methods for oil slick trajectory model. These classical methods can be used as basic tool for improvement of SAR oil slick trajectory model. The most widely used spreading formula is Mackay's algorithm. In Mackay's algorithm(Mackay, 1980), two expressions are used for the spreading of the thick and the total area of thick and thin slicks. For the thick slick, spreading consists of two parts, one a loss of area due to oil flowing from thick to thin slicks and second corresponding to Fay's algorithm. Fay's algorithm detects the change of area of the thick slick per time. These spreading mechanisms are function on the change of surface current movements.

The main objective of this study is to forecast the oil slick spreading along the coastal water of Malacca Straits.

1   Methodology

1.1   SAR image

SAR image was used in this study was the RADARSAT. The RADARSAT data were acquired at 26 October 1997. According to Mohd et al. (Mohd, 1999) oil spills occurred on 26 October 1997 due to collision between two ships, i.e. MT Orapin Global and MV Evoikos in Singapore. Mohd et al. (Mohd, 1999) reported that this collision caused 25000 tones of crude oil to be spilled into the sea.

This RADARSAT standard mode with C_{HH} band which covered the Malacca Straits between 102°16′ E to 103°48′ E and 1°16′N to 2°13′ N. The processing of the RADARSAT standard mode image is shown in Fig. 1. The processing consists on two parts. The first part involves with the automatic detection of oil slicks by utilizing of the textural algorithms and applying modeling the tidal current component velocities by Doppler

frequency models. The second part involves the effect of tidal current velocities on tracking the oil slick trajectory path.
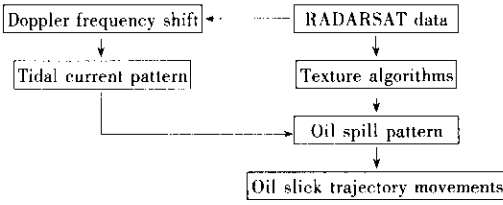

Fig.1 Block diagram of oil slick trajectory model

1.2 Oil slick detection model

The automatic detection of oil slick was done by using entropy algorithm. Entropy algorithm is one of texture algorithms which based on co-occurrence matrix(Haralick, 1979). The aim of this method is to characterize the stochastic properties of the spatial distribution of gray level in an image. Furthermore, the co-occurrence matrix depends not only on the spatial relationships of gray level but also on regional intensity background variation within the image. Texture analysis can be based on criteria derived from these co-occurrence matrices of local image variation(Milan, 1993).

According to Haralick(Haralick, 1979), Soren and Curtis(Soren, 1996) the window size of 7×7 gives more details on an image. As the window, size is used for producing the co-occurrence matrix for each input pixel. Spatial parameter is specified the relationship for a pixel to its neighbor to define the direction and distance for texture analysis. Local entropy texture algorithm derived from the first-order histogram of a 100×100 window is given as follows.

$$\text{Entropy} = -\sum_{j=0}^{k-1}\sum_{i=0}^{k-1} p(i)p(j)\ln[p(i)p(j)]. \tag{1}$$

Entropy is a measure of the amount of disorder. The greater the noise in the window, the higher the entropy value(Arai, 1991).

1.3 Modeling of truth current movement from tidal data

Due to the difficulties to obtained any real current measurements during the RADARSAT passing over the coastal waters of Malacca Straits, the tidal data were used to simulate the current water components. Then, the tidal current components were simulated from M_2 and its over-tide S_2 and assuming a rectilinear current, the speed can express as

$$U(t) = u'\cos\sigma t + u'_2\cos(2\sigma t - \beta); \tag{2}$$

$$V(t) = u'\sin\sigma t + u'_2\sin(2\sigma t - \beta), \tag{3}$$

where u', u'_2, are the amplitude of the M_2 and S_2, respectively, σ is the angular frequency of M_2 and β is the phase of S_2 relative to M_2, which is $\frac{\pi}{2}$(Hadi, 1996). The tidal current velocity can be divided into its x and y components as: $U = Ui(t) + Vj(t)$.

1.4 Doppler frequency model for current pattern simulation

The azimuth velocity component of surface current is modeled by estimating its displacement vector. The Doppler spectrum of the range compressed RADARSAT raw data is modeled by performing a fast Fourier transform(FFT) in azimuth direction. The current velocity for each pixel is divided into azimuth and range velocity. The azimuth velocity component of current movement is obtained by using a block-matching algorithm. The block-matching algorithm was performed to determine the best match between blocks in two successive windows. The difference of the positions in two windows is considered as the displacement vector

(Martian, 1997). Then, the azimuth component can be determined from the displacement vector Δx. It can be given by

$$\nu_{Cx} = \nu_{Ax}\left[1 - \left(1 - \frac{2\Delta x\delta x\nu_{Ax}}{\Delta f_i R_T \lambda}\right)^{-0.5}\right], \tag{4}$$

where δx is the pixel spacing in the azimuth direction, ν_{Ax} is the platform velocity, ν_{Ax} and λ denote the carrier wavelength and antenna speed in azimuth direction x, f_i are the look center frequency which estimated from Fourier transform, and R_T is the slant range. The current speed in the range direction has a different form. Using the Lagrangian interpolation from the four surrounding grid nodes(Fig. 2) derives the tidal current in azimuth direction and range direction, which modulated by sea truth data. The tidal current in azimuth and range direction, respectively can be given by

$$\left(\frac{\partial^2 V_{Cx}}{\partial^2 x}\right) = \frac{V_{i+1,j} - 2V_{i,j} + V_{i-1,j}}{L} \tag{5}$$
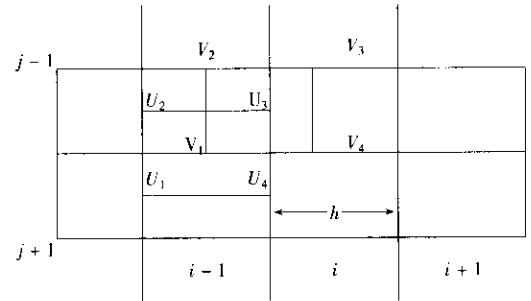

Fig.2 Sketch of tidal current detection by using Lagrangian model

1.5 Oil slick spreading model from RADARSAT

The oil slick was assumed to spread as an ellipse with the major axis in azimuth direction(Fig. 3), and minor axis in range direction. According to Lardner et al.(Lardner, 1988), the area of the ellipse is

$$A = \left(\frac{\pi}{4}\right)E_x E_y, \tag{6}$$

where $E_x E_y$ is the major and minor axis in the azimuth and range direction respectively. In order to estimate the value of major and minor axis, we are developed the algorithm as given by Lardner et al., 1988 to appropriate with RADARSAT image:

$$\Delta E_x = \Delta E_x + CV^{1.3}\left[\frac{2\nu_{sx}\nu_{an}^2}{\Delta f_i\lambda R_T}\right]0.75\left[\frac{f_i\lambda R_T}{2\nu_{an}^2}\right]^{0.25}. \tag{7}$$

Eq.(7) shows that the major axis of oil slick spreading can be based on the time variation along the azimuth direction. This time variation is function of Doppler frequency shift f_i and the velocity of oil slick along the azimuth direction (ν_{sx}), and current velocity V_{Cx} in azimuth direction.

The displacement along the range direction, ΔE_r can given by

$$\Delta E_r = C_2 \nu_{cy}^{1.3}\left[\frac{\nu_{ry}\sin\gamma R_T}{\nu_{an}^2}\right] \tag{8}$$

The spreading displacement of an oil particle at the azimuth and range direction (x, y) during a time dt can be given by

$$dx = S_x dt, \tag{9}$$

$$dy = S_y dt, \tag{10}$$

where

$$S = \frac{E_x^3 E'_x x^2 + E_y^3 E'_y y^2}{E_y E_x(E_x^2 y^2 + E_y x^2)}, \tag{11}$$

$$E'_x = dE_x/dt. \tag{11.1}$$

$$E'_y = dE_y/dt. \tag{11.2}$$
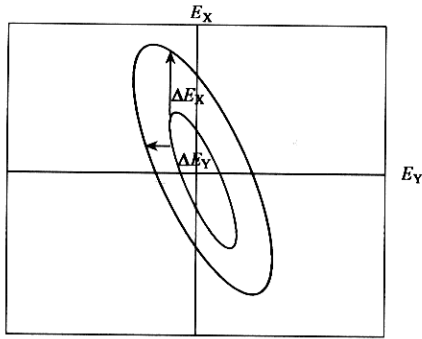
1.6 Trajectory model from RADARSAT

Fig.3   Elliptical spreading of oil slick

Once the tidal current velocities and the rate of spreading are modeled from RADARSAT image, it is easy to establish the trajectory model of oil slick. The parcel of oil slicks is divided into a large number of Lagrange parcels of equal size. At each time step, each parcel is given a diffusive and a convective displacement as follows. We assumed that the initial position(x_i , y_i) of spreading $S(t)_i$ in position of the ith parcel and the first guess position of oil slick spreading is S' (t + dt)$_{i+1}$. The velocity vectors are linearly interpolated in both space and time. The first guess position can be given by

$$S'(t + \Delta t)_{i+1} = S(t)_i + [V(S,t)]_{i+1,j}\Delta t, \qquad (12)$$

and final position can given by

$$S(t + \Delta t)_{i+1,j} = S(t)_{i,j+1} + 0.5[V(S,t) + $$
$$V(S',t + \Delta t)]_{i+1,j}\Delta t. \qquad (13)$$

Trajectories are terminated if they exit the model down to the water depth, but the advection continues along the surface. The integration time step Δt can vary during the simulation.

2   Results and discussion

The heavy dark spots are extended along the coastal water of Malacca Straits. These dark spots cover area with approximately 300 km (Fig. 4). The RADARSAT image also shows a speckle noises. This considers as the main problem in SAR data due to the constructive and destructive interference of coherent electromagnetic radiation. This is known as fading. The results of fading are manifested in SAR image as speckle. This is visually recognized as increased frequency light and dark pixels in what should be a restively homogenous grey level field(Ulaby, 1986).
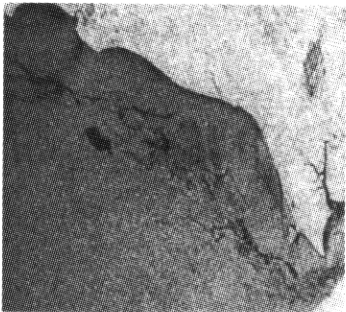

Fig.4   RADARSAT raw data

The dark oil slick spots are isolated from the surrounding sea waters(Fig.5). This result is the output of utilizing of entropy. This could be attributed to that entropy is a measure of uniformity in the image. Entropy measures the lack of spatial organization inside the oil slick region. Entropy inside the oil slick area is low when the texture of oil slick is smoother and more homogenous. Oil slick regions are represented by low entropies.
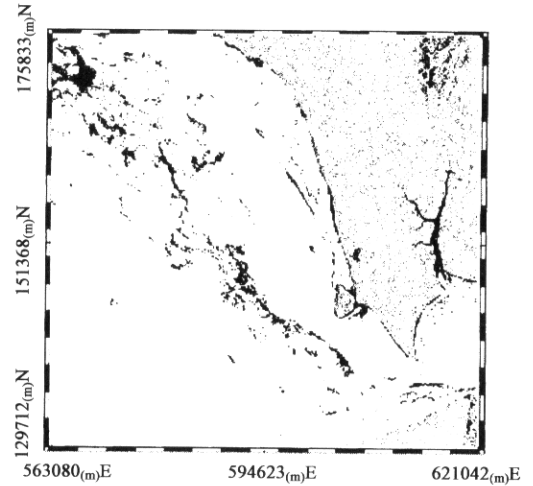

Fig.5   Output of entropy algorithm

Fig.6a shows that the simulated current velocity from RADARSAT image and Fig.6b shows that the simulated tidal current from tidal table during the RADARSAT pass over the coastal waters of Malacca Straits.
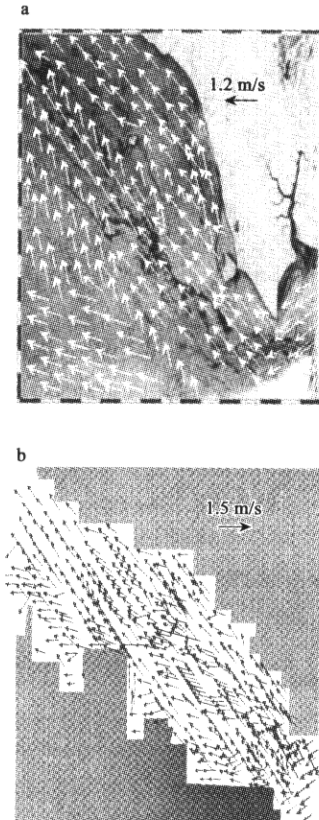

Fig.6   Tidal current velocity modeled from RADARSATT image (b) tidal current velocity simulated form ground and RADSRSAT data

The dominated current direction were towards the north direction with maximum current velocity of 1.2 m/s. This indicates that the strong current flow was in azimuth direction (Fig.6). Fig.7 shows a good correlation between simulated tidal current from RADARSAT image and ground data. The maximum velocity of M_2 is observed in the center away from the Singapore Straits. It is obvious that the M_2 is moved on an elliptical pattern(Fig.6a). This is due to the high effects of semi-diurnal tide on the water movements. The maximum M_2 speed was 1.4 m/s (Fig. 7), which approximately agreed with one simulated from RADARSAT data.
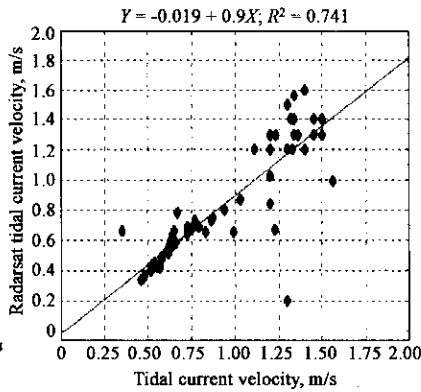

Fig.7   Regression model between RADARSA tidal current and ground tidal current

The tidal current direction tends to move along the azimuth direction. This may be because of that the M_2 tidal wave behaves like a standing wave. According to Azmy et al.(Azmy, 1992) the standing wave in the Malacca Straits is generated by two progressive waves traveling in opposite directions.

The effects of tidal current components on oil spills pattern can be observed from Figs. 8 and 9. It is obvious that the V components have good effects on oil spills length than U components. However, U components have good effects on oil spills width compared to V components. It can explain that due to the effects of V components, the oil spills tend to move towards the north direction. This means that the spreading of oil spills towards the west coast of Malaysia will be accelerated by U components effects.

It can be said that the oil spills movement on Malacca Straits is effected by the two tidal current components, U and V. This means that the spreading of oil spills towards the north could be faster due to the highest value of V components. It will be slower towards the west coast of Malaysia due to the lowest value of U components. This may be explained the larger length of oil spills as shown in Fig.5.

Fig.10a shows the simulated oil slick parcels at the same time of RADARSAT pass Fig.10b shows that 15% of oil spill parcels were deposited along the coastal waters of Johor Baru and 85% of oil parcels are still moving towards the azimuth direction. This occurs with 24 h. With 48 h 85% of oil parcels are deposited along the north coastline of western Peninsular Malaysia. This is because of the fact that the strongest V tidal current components in azimuth direction induced a high deposition of oil slick parcels in the same direction. The U tidal current components will assist to move the oil slick parcels towards the coastline.
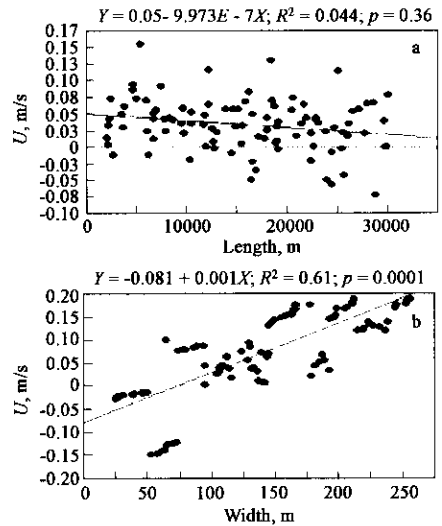

Fig.8   Regression model of U components effects on(a) oil spills length and (b) oil spills width
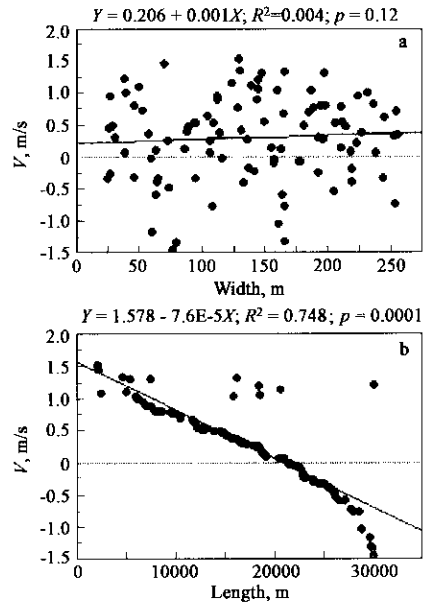

Fig.9   Regression model of V components effects on(a) oil spills width and (b) oil spills length

These results are agreed with the results of Figs. 8 and 9.

The results are not similar to Mohd et al.(Mohd, 1999). This is because that Mohd et al.(Mohd, 1999) assumed that the movement of oil spills based on convective-dispersive transport. The convective - dispersive transport required the depth averaged oil concentration, the dispersion coefficients, and vertical and horizontal velocity depth. Mohd et al.,(Mohd, 1999) could not be identified these items form RADARSAT image. The study of Mohd et al.,(Mohd, 1999) has not been shown any current velocities collected or modeled along the column water. Meanwhile, the oil spills pattern simulated by Mohd et al., (Mohd, 1999) have just been shown that the oil slick movement direction was towards the northwest direction, which is in agreement with the results of present study.
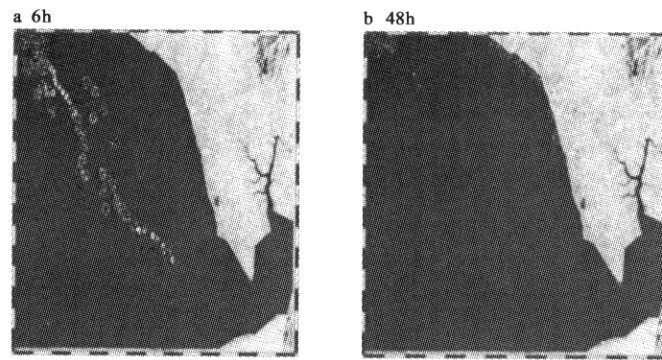
Fig.10   Results of oil slick trajectory movements

3　Conclusions

　　In conclusion, RADARSAT HH polarization image could be used as good tool for oil spill trajectory movements forecasting. This could be attributed to RADARSAT data which can model the current movement and easy detection of oil slick area by using entropy texture algorithms. The development of Fay's algorithm by using Doppler frequency shift model will assist for oil slick forecasting. The oil slick length ranged from 2 km to 300 km and oil slick width ranged from 50 m to 225 m. The spreading of oil parcels are noticed along the azimuth direction. This due to the effect of the tidal current V components which propagated along the azimuth direction with maximum speed of 1.4 m/s. The oil slick parcels approached the coastal water along the range direction within 48 h.

References:

Anne H, Solberg S, Geir S et al., 1999. Automative detection of oil spills in ERS SAR images[J]. IEEE Transactions on Geo & Remote Sen, 37(4): 1916—1924.

Arai K, 1991. GCP acquisition using simulated SAR and evaluation of GCP matching accuracy with texture features[J]. Int J Remote Sensing, 12(11): 2389—2397.

Azmy A R, Isoda Y, Yanagi T, 1992. M_2 tide and tidal current in straits of Malacca[Z]. Memories of the Faculty of Engineering. Ehime University, XII. 345—354.

Benelli G, Garzelli A, 1999. Oil-spills detection in SAR images by fractal dimension estimation[C]. Proceedings of IGARSS'99, 28 June—2 July, Homburg, Germany. Vol II. 1123—1126.

Bern T I, Moen S, 1992. Oil spill detection using satellite based SAR[R]. OCEANOR report No.: OCN-R92071.

Conners R W, Harlow C A, 1980. A theoretical comparison of texture algorithms [C]. IEEE Tr. on Pattern Analysis and Machine Intelligence, Vol PAMI-2, No. 3, May 1980.

Lardner R W, Lehr W J, Fraga R J et al., 1988. Residual currents and pollutant transport in Arabian Gulf[J]. Applied Math Modeling, 12: 379—390.

Hadi S, Dadang K, Michardja et al., 1996. Oil spill model of Makassa Straits [C]. Proceedings of the regional workshop on oil spill modeling, 31 May - 3 July, Puasan, Republic of Korea. 73—85.

Haralick R, 1979. Statistical and structural approaches to texture[J]. Proceedings of the IEEE, 67(5): 786—804.

Hovland H A, Johannessen J A, Digrances G, 1994. Slick detection in SAR images[C]. Proceedings of IGRASS 94, Pasadena,CA., August 8—12, 1994. 2038—2040.

Lopes A, Touzi R, Nezry E, 1990. Adaptive speckle filters and scene heterogeneity[J]. IEEE Transactions on Geo and Remote Sen, 28(6): 765—778.

Macky D, Stiver W, 1980. Testing of crude oil and petroleum products for environmental purposes[C]. Proceeding of oil spill conference, 1980. API, Washington, USA. 331—340.

Maged M M, Mansor S, Ibrahim Z Z, 1996. On the application of radarsoft to extract infrastructure details from RADARSAT[C]. Proceeding of Malaysian Remote Sensing Society conference on remote sensing and GIS. Crown Prince Hotel, Kuala Lumpur, Malaysia. 25—27 November, 1996.

Maged M, 2000. Finite element simulation of tidal current movements on Malacca Straits[C]. Proceeding of IGARSS'2000. Honolulu, Hawaii. 24—28 July 2000. Vol.II. 2966—2968.

Martian K, 1997. Detection and focused imaging of moving objects evaluating a sequence of single look SAR images[C]. Proceedings of 3rd international airborne remote sensing conference and exhibition. Copenhagen, Denmark. Vol. I: 393—400.

Michael D H, Olsen R B, Hoyt P et al., 1997. The ocean monitoring workstation experience gained with RADARSAT[C]. The geomatics in the ERS of RADARSAT '97 conference. Ottawa, Canada. 25—30 May, 1997.

Mohd I S, Salleh A M, Tze L C, 1999. Detection of oil spills in Malaysian waters from RADARSAT synthetic aperture radar data and prediction of oil spill movement[C]. Proceeding of 19th Asian conference. 23— 27 November, 1999. Hong Kong. Vol. 2: 980—987.

Milan S, Vachav H, Roger B, 1993. Image processing analysis and machine vission[M]. New York: Chapman and Hall Computing.

Soren R, Curtis W, 1996. Combining spectral and texture data in the segmentation of remotely sensed images[J]. J Photo Eng and Remote Sen, 62(2): 181—194.

Ulaby F T, Kouyate F, Brisco B et al., 1986. Textural information in SAR images[J]. IEEE Transactions on Geo & Remote Sen, 24(2): 233—245.

Wahl T, 1993. Oil spill detection using satellite based SAR[R]. Phase 1b completion report; Tech rep, Norwegian Defence Res.

Wesiteen K, Solberg A, Solberg R, 1993. Detection of oil spills in SAR images suing a statistical classification[C]. Proceedings of IGRASS 93, Tokyo, August 8—12. 943—945.

Wyrtki K, 1961. Physical oceanography of the South-East Asian waters[R]. NAGA Report, Vol. 2, Univ. Calif Scripps Inst. Ocean., La Jolla.